TELKOMNIKA Telecommunication, Computing, Electronics and Control
Vol. 18, No. 5, October 2020, pp. 2391~2400
ISSN: 1693-6930, accredited First Grade by Kemenristekdikti, Decree No: 21/E/KPT/2018
DOI: 10.12928/TELKOMNIKA.v18i5.14321

Developed approach for phase-based Eulerian video magnification

Haider Ismael Shahadi[1], Zaid Jabbar Al-allaq[2], Hayder Jawad Albattat[3]
[1]Electrical and Electronic Engineering Department, University of Kerbala, Iraq
[2,3]Communication Techniques Engineering Department, Al-Furat Al-Awsat Technical University, Iraq
[2]Technical Institute of Karbala, Al-Furat Al-Awsat Technical University, Iraq

Article Info

Article history:

Received Oct 13, 2019
Revised Apr 21, 2020
Accepted May 1, 2020

Keywords:

Eulerian video magnification
Lanczos-3 algorithm
Linear-based
Motion magnification
Phase-based

ABSTRACT

This paper proposes a modification approach for phased-based EVM in order to reduce the processing time without effect the quality of the magnified video. The proposed approach applies a resizing process on the input video using Lanczos-3 algorithm. Then, it decomposes video frames using steerable pyramid to obtain multi-scale frame with its orientation. Subsequently, the resulted frames are filtered by temporal filters for specific bands and the filtered frames are multiplied by a magnification factor. Now, both the magnified regions and the unmagnified regions for each frame are added together. Finally, reconstructing the produced magnified multi-scale frames using the inverse steerable pyramid. The experimental results show that superiority of the proposed approach compares to the conventional phase-based EVM in processing time, where the processing time reduction about 60-65%. Furthermore, this approach does not affect on the video quality, which maintain it in the boundary of the conventional Phase-based EVM.

Corresponding Author:

Haider Ismael Shahadi,
Electrical and Electronic Engineering Department,
University of Kerbala,
56001, Karbala, Iraq.
Email: corresp-author@mail.com

1. INTRODUCTION

Natural limitations of human vision system (HVS) to pick up important and useful signs make the video magnification techniques as a powerful key for several needs in health care [1-6], physical variations [7, 8], material behaviour detection [8], etc. The sensing of very slow motion or very small change in color is hard to be observed by naked eye of human. Liu et. al. [7] have introduced a motion and color magnification techniques depend on determining of the variations in motion or color via a robust investigation of trajectories. They gathered these trajectories to derive amplified motion or color traces for all pixels related to the registered reference frame. This technique requires a long processing time and it results a large noise in the magnified video frames. The method in [7] is based on Lagrangian and is computationally expensive, with long execution time (10 hours) because it relied on optical flow calculations [9] and a feature tracking algorithm. So that Hao et. Al [8] have proposed Eulerian-based video magnification (EVM) that is not follow the pixels motion such in Lagrangian approach. Therefore, it is faster than the Lagrangian-based method.

The first version of EVM utilizes Taylor series expansion that has a linear properties, therefore, it is called linear-based EVM algorithm [8]. The algorithm is relatively fast, but it does not supported high magnification factor as well noisy magnified video. The reason behind the high noise is due to the linearity,

where the noise is amplified by the same ratio of the magnification factor of the video frames. In order to reduce these drawbacks, Wadhwa et al. [10] have proposed a new Eulerian approach based on complex steerable pyramids [11, 12], which is stimulated by phase-based optical flow algorithms [13]. Their proposed approach has fewer artefacts and less noise as well as supports larger magnification factors compared to liner-based EVM (LB-EVM). Also, it can attenuate unwanted motion in case of color magnification. However, it is so complex and requires longer time to execute than the LB-EVM.

Several works have been published recently in order to enhance EVM, whether in linear based or phase-based [14]. Le Liu et al. [15] proposed an enhancement to EVM to reduce the noise in LB-EVM. So that authors have used a pixel-level motion analyzer to capture the spatio-temporal motion and then amplify it. The approach of motion utilizes an image warping is also used in order to amplify the motion in a video relying specific former motion mapping. Although the method improves noise performance in the processed video frames, the computation time is also increased and some specifications of magnified frames may be lost during image warping. Furthermore, the improve approach of LB-EVM also still failed in large magnification factor.

In [16], the authors have proposed an improved method of phase-based EVM (PB-EVM), which is called fast phase-based Eulerian video magnification (FPB-EVM). In this method, an image pyramid decomposition that employs Riesz-transform (R-T) has been used in the stage of multi-scale spatial decomposition. A video frames are first decomposed using Riesz pyramids that uses finite difference filters of two three-tap. Subsequently, the decomposed frames are filtered by invertible octave bandwidth filters. The authors in [16] claim that their approach can be using for real-time hidden motion visualization. Although this approach is faster than complex steerable in conventional PB-EVM, the main drawback is the Riesz pyramid fails to maintain the power of the input signal, which can cause low quality of the magnified video.

In [17], authors have proposed a method to solve problems of intensive processing time, and low video quality in EVM. The method is relying wavelet decomposition, and image de-noising. The authors have claimed that their method is superior over previous methods in terms of processing time reduction and noise elimination. However, all the tests that are listed in [17] have achieved for small magnification factors. This is because wavelet separate both noise and subtle motions in details bands that have small energy so that by amplifying these bands noise also magnified by the same ratio. According to literature, PB-EVM is best approach in terms of noise performances and large magnification factor [18]. The main problem is the long processing time.

This paper proposes an enhancement for phase-based-EVM (PB-EVM) in order to significantly reduce the processing time of the video magnification. The proposed approach reduces the processed data by resizing-down the input source video and then resizing-up the output frames of PB-EVM. The proposed resizing utilizes Lanczos-3 algorithm that is maintain the quality of the magnified video as it is in the conventional PB-EVM [19]. The rest of the paper is organized as: section 2 describes a PB-EVM approach. Section 3 illustrates the Lanczos-3 algorithm. Section 4 explains the proposed technique. Section 5 and section 6 explains the simulation results with discussion and comparison with the related work respectively. Finally, conclusions are given in section 7.

2. PHASE-BASED EULERIAN VIDEO MAGNIFICATION

The PB-EVM method has been developed by Wadhwa et al. [10]. It is based on complex steerable technique [11-13, 20], and phase-based optical flow [13]. The method attempts to overcome the drawbacks of LB-EVM such as support only small magnification factors and amplify noise linearly with increasing the magnification factor. The main drawback in this method is the long processing time.

The PB-EVM technique supports large magnification factors with significantly less noise than LB-EVM technique. The PB-EVM method does not increase the spatial noise because the method magnifies the phase instead of amplitudes for the interest regions. As a result, noise is translated rather than amplified when the amplification factor is increased. Therefore, this method increases the phase variations by a multiplicative factor to amplify the subtle motions.

Figure 1 shows the working mechanism stages of the PB-EVM technique. The technique starts by decomposing the video frames into multiple scales and orientation for different spatial-frequency bands. This is achieved by steerable pyramids that rely on Fourier analysis to analyse the image into sub-domains and routing. The basic functions of the transform are similar to Gabor wavelets, which are sinusoids windowed by a Gaussian envelope [11]. In the next stage, a temporal filter is applied to pass only the desired frequency bands. Then, the energy of the desired frequency bands is increased by multiplying filtered frame by an appropriate magnification factor. Then, the magnified bands are collected with the unmagnified bands for each frame. Finally, the magnified video frame is reconstructed by complex steerable pyramid reconstruction.

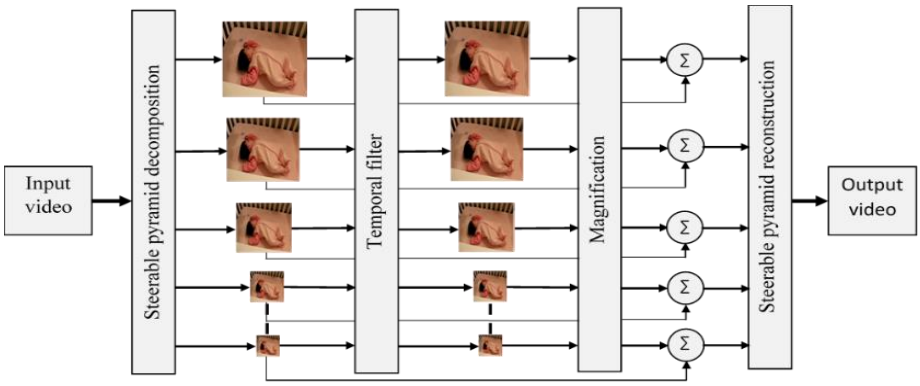

Figure 1. General structure of phase-based EVM [10]

The steerable pyramids are calculated through 2D Fourier transform (DFT) on all frames in the source video and subsequent applying the spatial filters, with varying size and direction. This is resulted a multi-dimensional and multi-directional linear analysis. Each level of the pyramid is a set of complex numbers. So that phase and amplitude are easily calculated for each resulted complex pair.

3. LANCZOS-3 INTERPOLATION ALGORITHM

The Lanczos-3 algorithm has been proposed by Cornelius Lanczos-3. It is an interpolation method used in image processing such as medical imaging [21] and video resizing [22]. The Lanczos-3 interpolation provides a smoothing to the image more than the bi-cubic algorithm. The interpolation kernel is considered in the algorithm, which is a multiplication of two SINC functions [23]. Figure 2 illustrates the Lanczos-3 kernel function that used in image resampling. The main formula of the resizing filter applies a Sinc function as shown in (1).

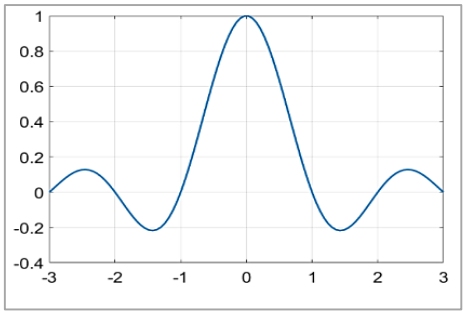

Figure 2. The function of Lanczos-3 kernel filter

$$L(x) = \begin{cases} 1 & x = 0 \\ \frac{a\sin(\pi x)\sin(\frac{\pi x}{a})}{\pi^2 x^2} & 0 < |x| < a \\ 0 & otherwise \end{cases} \quad (1)$$

where a is an integer that represents the filter size. A typical size of the kernel filter is 2 or 3. Consider a one-dimension vector which is having samples S_i, and let $S(x)$ be the interpolated value at a random argument x, then the resampled value of Lanczos kernel is given by (2).

$$S(x) = \sum_{i=|x|-a+1}^{|x|+a} S_i \, L(x-i) \quad (2)$$

In the 2D matrix, the resampled values of Lanczos kernel are calculated by the product of two 1D Kernel filters as shown in (3);

$$L(x,y) = L(x).L(y) \quad (3)$$

Consider a two-dimension S_{ij} which is defined at rows and column indices i and j respectively. The reconstructed or interpolated matrix is given by (4);

$$S(x,y) = \sum_{i=|x|-a+1}^{|x|+a} \sum_{j=|y|-a+1}^{|y|+a} S_{ij}\, L(x-i).L(y-j) \quad (4)$$

4. PROPOSED APPROACH

The proposed approach uses the same algorithm of the conventional PB-EVM. However, an important pre-processing and post-processing stages are added in such a way to overcome the problem of intensive execution time. Moreover, the quality of the magnified video is maintained without effecting. Figure 3 shows the main steps of the proposed approach.

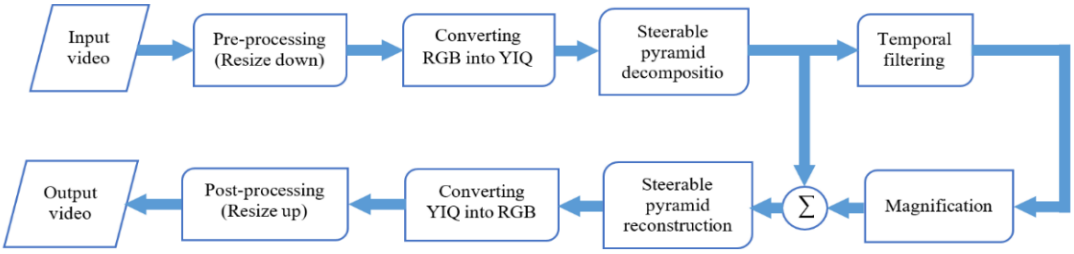

Figure 3. The block diagram of the proposed approach

The steps of the approach are as follows:

- The video file is read as AVI format, and then the frames of the video is resizing-down by 50% of the original height and width dimension. In this step, we employ Lanczos resampling method [24]. The resized frames' size of the resulted video is 25% of the source video.
- The next step after video resizing is the converting of all resulted video frames from RGB space into NTSC (or YIQ) space. The Y component represents the illumination information; I and Q represent the chrominance information. The NTSC color system is intended to income advantage of human response characteristics to the color. This step is done by applying (5) on all the frame of the resized video.

$$\begin{bmatrix} Y \\ I \\ Q \end{bmatrix} = \begin{bmatrix} 0.299 & 0.587 & 0.114 \\ 0.596 & -0.274 & -0.322 \\ 0.211 & -0.523 & 0.312 \end{bmatrix} \begin{bmatrix} R \\ G \\ B \end{bmatrix} \quad (5)$$

- The third step in the approach is applying the steerable pyramid decomposition on each layer (Y, I, and Q) from the video frames individually. The decomposition is used to factorize the video frames into scalable images for different levels of decomposition. The steerable pyramid is a transform that analyses an image based on spatial scale, orientation, and position. In this process 2-D discrete Fourier transform (DFT) is applied over all the resized video frames in YIQ space. Subsequently, the spatial filters of different size and orientation are applied. The steerable pyramid produces a linear multi-scale and multi-orientation decomposed image. Each level from the output is array of complex numbers, which consists of amplitude and their phase for each element in the array.
- The resulted bands from the previous step entered to temporal filter. In order to pass only the interest bands of frequencies to amplify them in the next step.
- In this step, the resulted band coefficients from the temporal filter are multiplied by the magnification factor to amplify the interested temporal frequencies.
- Subsequently, the magnify bands combine with the original bands that resulted from the spatial decomposition in step 3.
- Inverse of steerable complex pyramid is applied on the results of the previous step to reconstruct the video frames after amplification in YIQ space.
- Subsequently, convert frames from YIQ space into RGB space to obtain the original color of video. This step is done by applying (6) on all the frame of the video.

$$\begin{bmatrix} R \\ G \\ B \end{bmatrix} = \begin{bmatrix} 1 & 0.956 & 0.619 \\ 1 & -0.272 & -0.647 \\ 1 & -1.106 & 1.703 \end{bmatrix} \begin{bmatrix} Y \\ I \\ Q \end{bmatrix} \quad (6)$$

– Finally, the output video from the previous step is resizing-up by 200 % of height and width of the frames to get the same original size of the source video by using Lanczos-3 resampling method.

5. RESULTS AND DISCUSSION

This section presents experimental results to compare the modified PB-EVM approach with the conventional PB-EVM approach. Figure 4 shows the used videos in our tests, which include: Baby1 video with dimension 960×544×3×301 and a frame rate of 30 frame per second(fps), Eye video with dimension 1152×896×3×140 and a frame rate of 30 fps, Baby2 video with a dimension 640×352×3×900 and a frame rate of 30 fps, Baby3 video with a dimension 1280×720×3×222 and a frame rate of 30fps. All the videos except Baby3 can be found on the websit of the MIT [25]. The Baby3- video has been recorded by the Preterm department- central child hospital -Iraq and the baby has casualty viral hepatitis.

In order to compare the proposed approach over the conventional one, we measure the quality of the resulted videos from each approach. The quality measurement is achieved by measuring Peak signal-to-noise ratio (PSNR) according to (7) for each frame;

$$PSNR = 10 \log \frac{255^2}{MSE} \quad (7)$$

$$MSE = \frac{1}{N \times M} \sum_i^N \sum_j^M \left(I_{i,j} - Ia_{i,j}\right)^2$$

where, MSE is the mean square error, I and Ia are the original and the amplified frames respectively, M and N are the frame dimensions.

In addition to PSNR, maximum absolute error (MAXERR) is also calculated in the tests that represents the absolute maximum squared deviation of the input to the output video frames. Furthermore, L2RAT is also used to measure the ratio of the squared norm of the output to the input video frames. We have implemented our tests by applying octave bandwidth of complex steerable pyramids that have wide spatial support. Several groups of tests have been achieved as illustrated in Figure 4.

(a) (b) (c) (d)

Figure 4. The source videos that used in the experimental results (a) Baby1 (b) Eye (c) Baby2 (d) Baby3

a. In the first group of tests, Baby1 video as shown in Figure 4 (a) has been used as a source video. The goal of this group of tests is to detect the weak breathing of the baby by magnifying the subtle motion of the region around the chest and abdominal area. Infinite impulse response (IIR) has been used as temporal filter with three sets of different tests as follows:

– Set1: in this set of tests, the value of sigma is changed as {1, 3, 5, 7, and 10}. While, the frequency boundaries of the band-pass temporal filter are 0.1 Hz for the lowest frequency and 0.4 Hz for the highest frequency. That mean the breathing happens 6-24 times per minute. The magnification factor is fixed with value equals to 20. Table 1 shows the experimental results that illustrate comparison between conventional and proposed approaches. As shown in the table, the increasing of sigma value leads to increase the quality of magnified video, however, the execution time increases too. The table shows the superiority of the proposed over the conventional in reducing the processing time upto 60% with maintaining the video quality.

– Set2: In this set of tests, α varies with values {30, 40, 50, 60, and 100} and fixed value of sigma (5). The frequency boundaries of the band-pass temporal filter are {0.1-0.4Hz}. Table 2 shows the comparison between the proposed and conventional approaches. The results of the table show the superiority of the proposed over the conventional method in reducing the execution time by more than 60% and keeping the video quality within a conventional PB-EVM limit. Figure 5 shows samples of the amplified frames with respect to the source frames for both the proposed and conventional approaches, where α=100 and sigma = 5. From Figure 5 we see that the amplified frames using the proposed method have quality

resemble to the amplified frames using the conventional method with execution time less than half of that required in the conventional approach. Figure 6 show comparison in PSNR values between the conventional and proposed approach for Baby1 video frames. Furthermore, the survival of the video quality of the proposed approach remains close with the conventional method.

Table 1. Set1 results for the proposed based PB-EVM for Baby1 at α=20

Sigma value	Conventional PB-EVM [10]					Proposed improved PB-EVM				
	Execution Time	PSNR	MSE	MAXEER	L2RAT	Execution Time	PSNR	MSE	MAXEER	L2RAT
1	218.27	32.15	39.65	130.30	0.9993	82.72	32.25	40.36	124.79	0.9989
3	219.67	32.51	36.45	128.82	0.9994	78.92	32.49	36.79	123.96	0.9992
5	225.23	32.79	34.22	125.26	0.9994	85.36	32.74	34.72	121.95	0.9992
7	223.49	32.99	32.65	123.55	0.9994	84.18	32.99	33.37	120.10	0.9992
10	230.94	33.21	31.04	120.94	0.9995	85.44	33.09	32.06	118.08	0.9993

Table 2. Set2 results for the proposed based PB-EVM for Baby1 at sigma = 5

Magnify factor	Conventional PB-EVM [10]					Proposed improved PB-EVM				
	Execution Time	PSNR	MSE	MAXEER	L2RAT	Execution Time	PSNR	MSE	MAXEER	L2RAT
α = 30	225.78	31.42	46.89	137.78	0.9993	85.79	31.49	46.24	125.32	0.9989
α = 40	226.86	30.08	63.81	143.69	0.9989	86.20	30.18	62.72	128.48	0.9986
α = 50	228.22	28.91	83.52	144.84	0.9985	86.72	28.97	82.95	133.61	0.9983
α = 60	227.28	27.99	103.35	143.48	0.9980	86.36	27.99	103.58	138.11	0.9979
α = 100	229.44	24.07	282.43	155.17	0.9958	87.18	24.07	282.43	155.17	0.9958

(a)

(b)

(c)

Figure 5. Samples of the experimental results for Baby1 at α=100 and sigma = 5 (a) source frames, (b) amplified frames using conventional PB-EVM, (c) amplified frames using proposed based PB-EVM

– Set3: In this set of tests, the boundary frequencies of the band-pass temporal filter have been changed with values {0.1-0.4, 0.15-0.4, 0.2-0.38} Hz. While use fixed value for sigma 5, and the magnification factor α is 20. Table 3 shows the experimental results for the proposed and conventional approaches.

From the results of the table we can see that the boundary frequencies {0.2-0.38 Hz} give higher quality than the other frequency limits. Also, it is clear that the proposed method is superior over the conventional method in reducing the implementation time by more than 61% with maintaining the magnified video quality.

Table 3. Set3 results for the proposed based PB-EVM for Baby1 at α=20 and sigma = 5

Band-pass (Hz) value	Conventional PB-EVM [10]					Proposed improved PB-EVM				
	Execution Time	PSNR	MSE	MAXEER	L2RAT	Execution Time	PSNR	MSE	MAXEER	L2RAT
0.09-0.4	223.15	35.65	17.71	111.37	0.9998	84.79	35.95	16.52	98.01	0.9998
0.15-0.4	220.06	38.09	10.09	95.72	0.9998	81.42	38.59	8.99	91.53	0.9998
0.2-0.38	204.64	40.38	5.95	72.37	0.9999	77.76	40.86	5.33	70.12	0.9999

b. In the second group of tests, Eye video as shown in Figure 4 (b) is used as a source video. The goal here is to magnify the subtle motion happens in the eye muscle and its capillaries. Finite impulse response (FIR) has been used as temporal filter in three different sets of tests that are explained below.

– Set1: Sigma is changed with values {1, 3, 4, 7, 10}. While, the boundary frequencies of the band-pass temporal filter values are {30-50 Hz} with α = 75. Table 4 shows the experimental results for the proposed and conventional methods. As shown in the table, the increasing of sigma leads to increasing the quality of magnified video and execution time. Also, we can clearly see the superiority of the proposed method over the conventional method in reducing the execution time in around 50% with maintaining the video quality. Figure 7 show comparison in PSNR values between the conventional and proposed approach for the magnified eye frames. From this figure it is clear that the video frame quality of the proposed approach remains close with the conventional method.

Table 4. Set1 results for the proposed based PB-EVM for Eye at α=75

Sigma value	Conventional PB-EVM [10]					Proposed improved PB-EVM				
	Execution Time	PSNR	MSE	MAXEER	L2RAT	Execution Time	PSNR	MSE	MAXEER	L2RAT
1	205.58	29.52	72.65	200.78	0.9899	103.60	29.55	72.54	199.42	0.9899
3	205.79	29.69	69.72	201.34	0.9915	106.92	29.77	68.99	198.19	0.9913
4	211.98	29.79	68.25	200.73	0.9917	102.80	29.88	67.12	195.66	0.9915
7	245.46	29.98	65.29	197.48	0.9919	120.64	30.09	63.69	194.33	0.9918
10	251.95	30.11	63.38	195.35	0.9920	121.74	30.24	61.89	192.75	0.9918

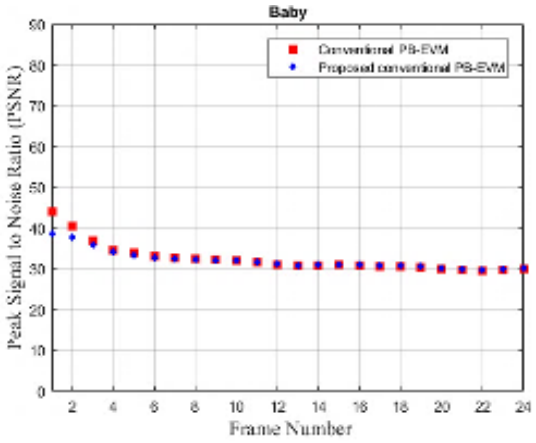

Figure 6. Comparison between the proposed and conventional approaches for Baby1 video at α=20

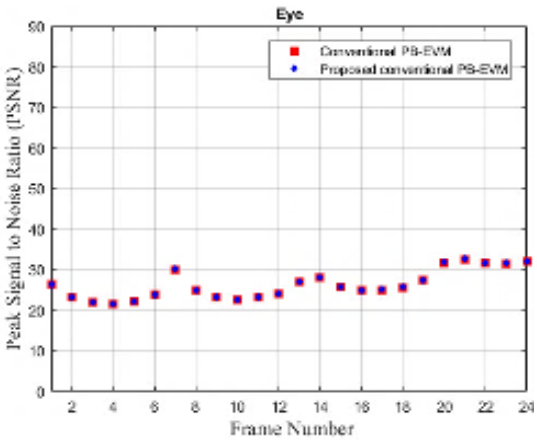

Figure 7. Comparison between the proposed and conventional approaches for Eye video at α=75

– Set2: the magnification factor α is varied with values {60, 85, 90, 100} and a fixed value of the sigma = 4. The frequency boundaries of the band-pass temporal filter are {30-50 Hz} for all values of α. Table 5 shows the experimental results of PB-EVM method for the proposed and conventional.

Through the results of the table we clearly see that superiority of the proposed method over the conventional method in reducing the processing time by around 50%, while the video quality keeps within conventional PB-EVM limits.

Table 5. Set2 results for the proposed based PB-EVM for Eye at Sigma = 4

Magnify factor	Conventional PB-EVM [10]					Proposed improved PB-EVM				
	Execution Time	PSNR	MSE	MAXEER	L2RAT	Execution Time	PSNR	MSE	MAXEER	L2RAT
α = 60	211.73	30.58	56.94	199.23	0.9929	108.89	30.69	55.79	199.89	0.9926
α = 85	210.41	29.35	75.56	209.30	0.9909	106.36	29.47	74.49	204.15	0.9907
α = 90	212.75	29.15	79.09	210.14	0.9907	105.65	29.25	78.05	205.50	0.9904
α = 100	211.15	28.79	85.93	213.21	0.9898	110.05	28.86	84.90	209.63	0.9896

– Set3: the boundary frequencies for the band-pass temporal filter is use with various values {30-35, 40-50, 50-60} Hz. While use fixed value for Sigma = 4 and α=75. Table 6 shows the experimental results of the proposed and conventional approaches by using Eye video as input. Again, the table shows that the proposed approach superior in terms of time reduction over the conventional, where the required processing time for the proposed is about half of that in the conventional one without effect the quality of the magnified video.

Table 6. Set3 results for the proposed based PB-EVM for Eye at Sigma = 4 and α=75

Band-pass (Hz) value	Conventional PB-EVM [10]					Proposed improved PB-EVM				
	Execution Time	PSNR	MSE	MAXEER	L2RAT	Execution Time	PSNR	MSE	MAXEER	L2RAT
30-35	208.39	29.43	74.17	199.83	0.9924	106.67	29.49	73.17	192.82	0.9921
40-50	208.22	30.59	56.66	194.15	0.9937	108.84	30.67	94.60	188.07	0.9923
50-60	214.06	31.99	41.07	175.20	0.9946	107.36	32.04	76.25	167.60	0.9942

c. In the third group of tests, Baby2 video as shown in Figure 4 (c) is use: The goal here is to magnify head movement resulting from the child's breathing. IIR has been used as temporal filter, and the magnification factor varies with values {20, 40, 60, 80, 100 and 150} and fixed value of sigma (5). The frequency boundaries for the band-pass temporal filter are {0.3-0.5 Hz}. Table 7 shows the comparison between the proposed and conventional approaches. The time reduction in the proposed method is about 54% compare to the conventional one with maintaining the magnified video quality.

Table 7. Comparisons between the proposed and conventional PB-EVM for Baby2 video

Magnify factor		α = 20	α = 40	α = 60	α = 80	α = 100	α = 150
Conventional PB-EVM [10]	Execution Time	225.69	226.39	227.92	228.35	228.82	229.95
	PSNR	35.77	33.17	31.35	30.05	29.06	27.38
	MSE	18.56	37.22	57.96	77.62	95.62	135.13
	MAXEER	63.50	88.50	107.74	119.90	128.85	146.40
	L2RAT	0.9982	0.9978	0.9974	0.9970	0.9966	0.9957
Proposed improved PB-EVM	Execution Time	103.81	104.13	104.84	105.03	105.25	105.77
	PSNR	34.04	32.22	30.39	29.66	28.03	26.84
	MSE	25.64	39.01	59.44	70.32	110.91	146.22
	MAXEER	72.42	93.93	111.40	122.21	128.87	138.32
	L2RAT	0.9979	0.9975	0.9970	0.9966	0.9957	0.9948

d. Baby3 video as shown in Figure 4 (d) has been used in the fourth group of tests. The baby in this video has viral hepatitis and has difficulty breathing. Therefore, the goal of magnification is to monitor his breathing. IIR is used as a temporal filter, α with various values {30, 60, 80, 100, and 150}. While, the values of boundary frequencies for the band-pass temporal filter are {0.2–0.4 Hz} and fixed value of sigma is used, Sigma = 5. Table 8 shows the experimental results for the proposed and conventional methods. The time reduction in the proposed one is around 70% compare to the conventional one with maintaining the magnified video quality.

Table 8. Comparisons between the proposed and conventional PB-EVM for Baby3 video

Magnify factor		α = 30	α = 60	α = 80	α = 100	α = 150
Conventional PB-EVM [10]	Execution Time	231.37	232.52	232.73	247.89	245.54
	PSNR	32.88	29.29	28.06	27.19	25.73
	MSE	37.86	85.78	112.69	136.44	188.87
	MAXEER	135.28	164.80	175.65	182.16	189.21
	L2RAT	0.9994	0.9983	0.9975	0.9967	0.9946
Proposed improved PB-EVM	Execution Time	71.72	72.08	72.14	74.36	73.66
	PSNR	32.74	29.22	27.99	27.13	25.69
	MSE	38.56	86.60	113.56	137.28	189.66
	MAXEER	129.74	161.92	173.01	180.15	189
	L2RAT	0.9993	0.9983	0.9975	0.9967	0.9946

6. COMPARISON WITH THE RELATED WORK

This section compares between the proposed method and the related methods in the literature. Table 9 shows the execution time and video quality in terms of PSNR for different methods. It is easy to see the significant reduction in processing time of the proposed method over all others. Furthermore, it is maintaining video quality same as in conventional PB-EVM method that have the superiority in terms of video quality compare to the other method in literature. In all the test of Table 9, Baby1 has been used as a video source file. Figure 8 shows an example of the magnified video frame using different magnification techniques at α=20. The figure shows the difference in frame quality visually.

Table 9. Comparison of the proposed and other relevant video magnification methods

Input Videos	Methods									
	LB-EVM [8]		Enhance EVM [15]		Conventional PB-EVM [10]		FPB-EVM [16]		Proposed PB-EVM	
	Execution Time	PSNR	Execution Time	PSNR	Execution Time	PSNR	Execution Time	PSNR	Execution Time	PSNR
Baby1	85.67	31.75	101.32	34.91	225.23	32.79	117.45	31.91	85.36	32.74

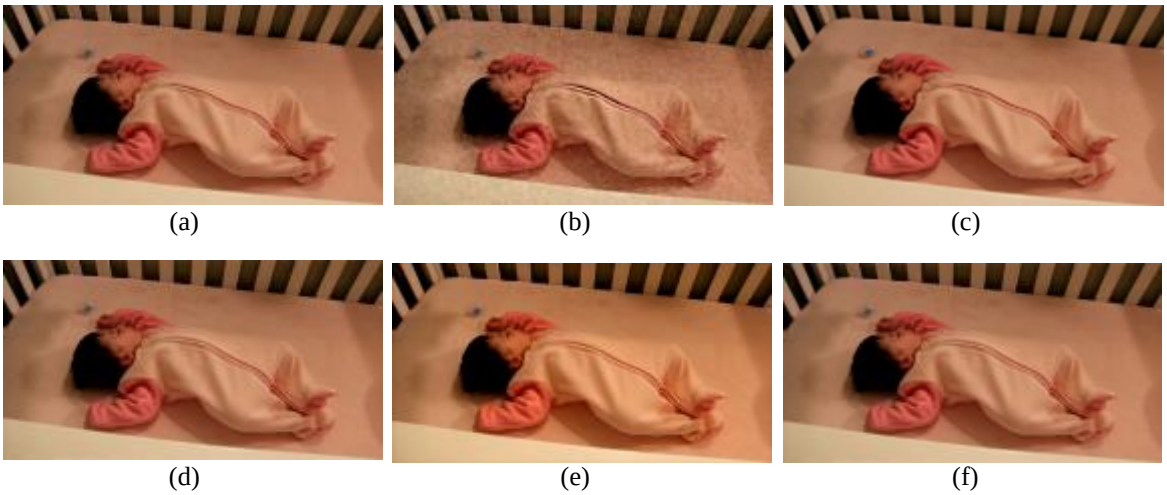

Figure 8. Magnified videos using different magnification techniques; (a) source frames, b) amplified frames based on LB-EVM approach, (c) amplified frames based on E2VM approach, (d) Amplified frames based on conventional PB-EVM approach, (e) amplified frames based on FPB-EVM approach, and (f) amplified frames based on proposed PB-EVM approach

7. CONCLUSIONS

This paper presents an effective modification for PB-EVM method in order to reduce the required processing time. The proposed technique uses the Lanczos algorithm that based on kernel filter to resize-down data of the source video before processing and resize-up after processing. This algorithm maintains the quality of the amplified video within PB-EVM quality limits. Experimental results show that the required processing time is reduced by more than half. Moreover, the comparison with the related method shows the superiority of the proposed over the others in terms of reduction both processing time and magnified noise.

The proposed technique supports large magnification factor with minimum noise amplification resemble to PB-EVM. Therefore, it can be used easily to detect invisible changes in the videos to be clearly perceptible to a nick eye. So that several applications can employ our technique such as in health care, engineering and biological microscopy.

REFERENCES

[1] Poh M. Z., McDuff D. J., Picard R. W., "Non-contact, automated cardiac pulse measurements using video imaging and blind source separation," *Optics Express*, vol. 18, no. 10, pp. 10762-10774, 2010.

[2] Poh M. Z., McDuff D. J., Picard R. W., "Advancements in Noncontact, Multiparameter Physiological Measurements Using a Webcam," IEEE Transactions on Biomedical Engineering, vol. 58, no. 1, pp. 7-11, 2011.

[3] Verkruysse W., Svaasand L. O., Nelson J. S., "Remote plethysmographic imaging using ambient light," *Optic Express*, vol. 16, no. 26, pp. 21434-214345, 2008.

[4] Balakrishnan G., Durand F., Guttag J., "Detecting pulse from head motions in video," P*roceedings of the IEEE Computer Society Conference on Computer Vision and Pattern Recognition*, Portland, OR, USA: IEEE; 2013.

[5] Al. Naji A., Chahl J., "Contactless cardiac activity detection based on head motion magnification," I*nternational Journal of Image and Graphics*, vol. 17, no. 1, pp. 1-18, 2017.

[6] He X., Goubran R. A., Liu X. P., "Wrist pulse measurement and analysis using Eulerian video magnification," *3rd IEEE EMBS International Conference on Biomedical and Health Informatics*, pp. 41-44, 2016.

[7] Liu C., Torralba A., Freeman W. T., Durand F., Adelson E. H., "Motion magnification," *ACM Digital Library*, vol. 24, no. 3, pp. 519-526, 2005.

[8] Wu H. Y., Rubinstein M., Shih E., Guttag J., Durand F., Freeman W., "Eulerian video magnification for revealing subtle changes in the world," *ACM Digital Library*, vol. 31, no. 4, pp. 1-8, 2012.

[9] Sigit R., Roji C. A., Harsono T., Kuswadi S., "Improved echocardiography segmentation using active shape model and optical flow," *TELKOMNIKA Telecommunication Computing Electronics and Control*, vol. 17, no. 2, pp. 809-818, 2019.

[10] Wadhwa N., Rubinstein M., Durand F., Freeman W. T., "Phase-based video motion processing," *ACM Digital Library*, vol. 32, no. 4, 2013.

[11] Portilla J., Simoncelli E. P., "A Parametric Texture Model Based on Joint Statistics of Complex Wavelet Coefficients," *Int J Comput Vis.*, vol. 40, no.1, pp. 49-71, 2000.

[12] Simoncelli E. P., Freeman W. T., Adelson E. H., Heeger D. J., "Shiftable Multiscale Transforms," *IEEE Transactions on Information Theory*, vol. 38, no. 2, pp. 587-607, 1992.

[13] Gautama T., Van Hulle M. M., "A phase-based approach to the estimation of the optical flow field using spatial filtering," *IEEE Trans Neural Networks*, vol. 13, no. 5, pp. 1127-1136, 2002.

[14] Shahadi H. I., Al-allaq Z. J., Albattat H. J., "Efficient denoising approach based Eulerian video magnification for colour and motion variations," *International Journal of Electrical and Computer Engineering (IJECE)*, vol. 10, no. 5, pp. 4701-4711, 2020.

[15] Liu L., Lu L., Luo J., Zhang J., Chen X., "Enhanced Eulerian video magnification. In: Image and Signal Processing (CISP)," *2014 7th International Congress on. Dalian*, China: IEEE, 2014.

[16] Wadhwa N., Rubinstein M., Durand F., Freeman W. T., "Riesz pyramids for fast phase-based video magnification," *2014 IEEE International Conference on. Santa Clara*, CA, USA: IEEE; 2014.

[17] Al-Naji A., Lee S. H., Chahl J., "An efficient motion magnification system for real-time applications," *Mach Vis Appl Springer*, vol. 29, no. 4, pp. 585-600, 2018.

[18] Shahadi H. I., Albattat H. J., Al-Allaq Z. J., Thahab A. T., "Eulerian video magnification: A review," *Indonesian Journal Electrical Engineering Computing and Science.*, vol. 18, no. 2, pp. 799-811, 2020.

[19] Al-allaq Z. J., Shahadi H. I., Albattat H. J., "Powerful and Low Time Phase-Based Video Magnification Enhancing Technique," *2019 4th Scientific International Conference Najaf (SICN)*, 2019.

[20] Freeman W., Adelson E. H., Heeger D., "Motion without movement," *ACM SIGGRAPH Computer Graphics*, vol. 25, no. 4, pp. 27-30,1991.

[21] Moraes T., Amorim P., Silva J., Pedrini H., "3d lanczos iterpolation for medical volumes," *15th International Symposium on Computer Methods in Biomechanics and Biomedical Engineering*, 2018.

[22] Yoo D. S., Chang J., Park C. H., Kang M. G., "Video resampling algorithm for simultaneous deinterlacing and image upscaling with reduced jagged edge artifacts," *EURASIP Journal on Advances in Signal Processing*, vol. 88, pp. 1-24, 2013.

[23] Parsania P. S., Virparia P. V., "A comparative analysis of image interpolation algorithms," *International Journal of Advanced Research in Computer and Communication Engineering*, vol. 5, no. 1, pp. 29-34, 2016.

[24] Madhukar B. N., Narendra R., "Lanczos resampling for the digital processing of remotely sensed images," Proceedings *of International Conference on VLSI, Communication, Advanced Devices, Signals & Systems and Networking (VCASAN-2013)*, 2013.

[25] Massachusetts Institute of Technology, "Vidio Magnification," 2010. [Online]. Available: http://people.csail.mit.edu/mrub/vidmag/